1981-11

Calculation of optical extinction from aerosol spectral data

Schacher, G.E.

Calculation of optical extinction from aerosol spectral data

G. E. Schacher, K. L. Davidson, C. W. Fairall, and D. E. Spiel

A major overwater experiment, MAGAT–80, has been undertaken to verify the use of aerosol spectrometers to calculate optical extinction in the marine boundary layer. Techniques for data averaging and for extrapolation to large particle sizes are described. Coincident optical, aerosol, and meteorological measurements by ship, aircraft, and an overwater optical range show that aerosol spectra can be used to predict extinction to within 40%.

I. Introduction

Particle counters can be used to determine the extinction of optical radiation by the atmospheric aerosol. The most commonly used are optical counters, where the scattering of a light beam is used to measure particle size spectra. To size successfully the particles passing through a light beam, sophisticated electronic circuitry is needed to measure both the height and width of the scattered light pulses. If the index of refraction of the particles is known, the scattered light intensity is determined by the particle size. Ideally, if particle size is to be determined from a single scattered pulse, the particle index of refraction must be known. (The refractive-index sensitivity can be reduced considerably by using forward-scattering geometry.) The relationships are multivalued for certain ranges of scattered light intensity. Thus determining aerosol spectra, and ultimately optical extinction, from optical counters is neither simple nor straightforward. For this reason, the credibility of this technique is still controversial.

The Environmental Physics Group of the Naval Postgraduate School (NPS), The Propagation Division of the Naval Ocean Systems Center (NOSC), and The Atmospheric Physics Branch of the Naval Research Laboratory (NRL) have expended considerable effort to answer this question.[1] This paper describes the technique and the results of optical and spectrometer intercomparisons performed by NPS which demonstrate that the spectrometers can be successfully used in the natural regime.

G. E. Schacher and K. L. Davidson are with U.S. Naval Postgraduate School, Environmental Physics Group, Monterey, California 93940; the other authors are with BDM Corporation, Monterey, California 93940.

Received 1 May 1981.
0003-6935/81/223951-07$00.50/0.

II. Spectrometer Details

Most of the data reported here were obtained by shipboard measurements with NPS Particle Measurement System's (PMS) spectrometers, models ASASP-300 and CSASP-100. They are sensitive to particles with radii from ~0.1 to 3 μm and 0.5 to 15 μm, respectively. The ASASP is divided into four ranges of fifteen bins each and the CSASP into two ranges of fifteen bins each. The arrangements of the size bins for these two spectrometers are shown in Fig. 1. Aircraft measurements were made with the NOSC Particle Measurement System's ASSP spectrometer, which is sensitive to radii from 0.28 to 14 μm. The ASSP size range is divided into four ranges of fifteen bins each.

The shipboard spectrometers were operated in conjunction with a DAS-32 data acquisition system. For almost all measurements the slowest DAS rate was used (a 40-sec data sample for each successive range cycle). The data output is accumulated in the memory of a Hewlett-Packard 9825S computer to obtain 30-min averages. A DAS-32 data acquisition system and 9825 computer are also used for the aircraft work, however, data are accumulated for 2-sec periods and stored without preprocessing.

Since the intensity of scattered light is not a monotonic function of particle size, the spectrometers have size regions where sizing uncertainty exists called ambiguity zones.[2] Spectrometer responses as a function of particle diameter, after Pinnick and Auvermann,[2] are shown in Fig. 2. The curves are for particle indices of refraction of 1.33 and 1.5. The size regions where ambiguities occur are easily seen and are indicated by shaded regions in the figure. The ambiguity zones are also indicated in Fig. 1 to show which PMS size bins are affected. If marine aerosol droplets have an index of refraction near 1.33 (pure water) all of Range-0 of the ASASP spectrometer is affected by ambiguity caused sizing uncertainties. Range-1 of the CSASP is also

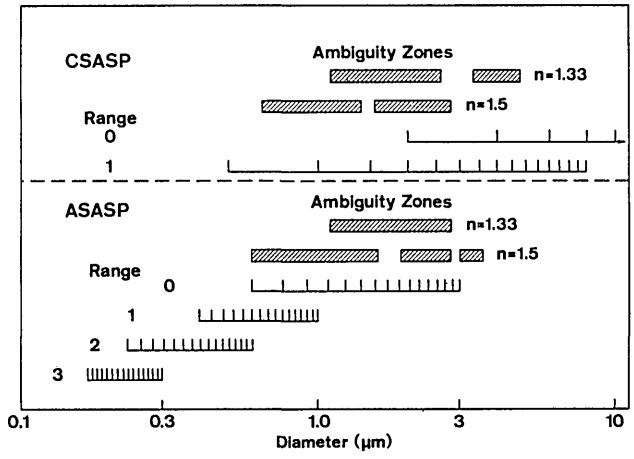

Fig. 1. ASASP and CSASP spectrometer bin configurations. Bins for each range are shown as boxes. Size ranges for ambiguity zones are indicated by shaded areas.

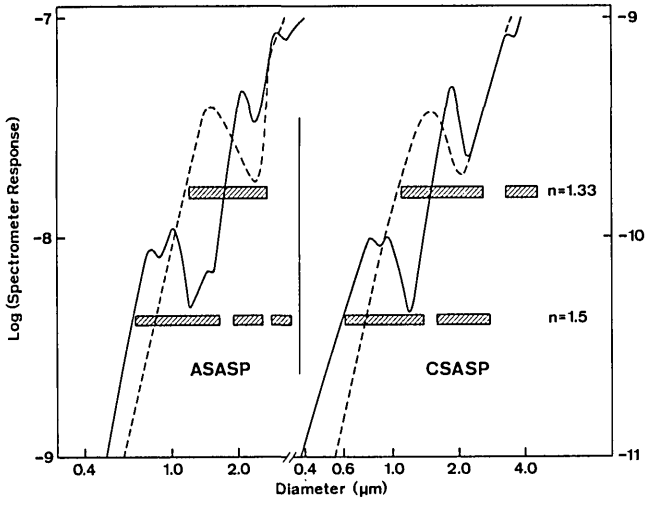

Fig. 2. Spectrometer response as a function of particle radius for indices of refraction of 1.33 and 1.5 for ASASP and CSASP spectrometers. Shaded areas ambiguity zones.

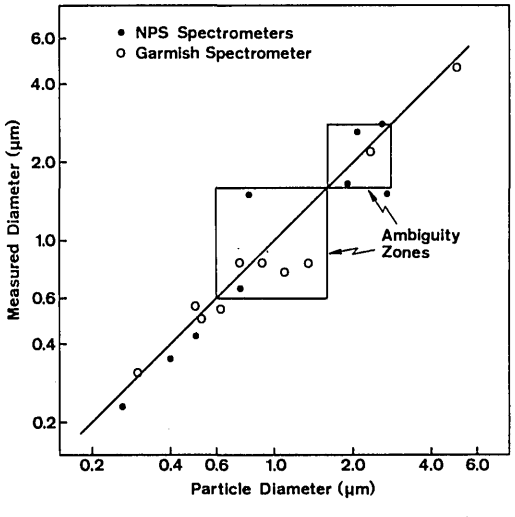

Fig. 3. Particle size calibrations for NPS and Garmisch spectrometers. Solid line shows correct sizing. Squares enclose ambiguity zones.

affected, but, because of the great bin width, reasonable size discrimination remains.

It has been our experience with the spectrometers that the smallest size bins for each range often show an elevated number of counts. The first three bins in each range of the ASASP and the first bin in each range of the CSASP are most commonly affected. Because the various ranges overlap, the smallest size bins for each range are redundant except for ASASP range 3. Clearly there is a wide choice as to which size bins to include in the analyses to deduce the aerosol spectra. The method we have chosen has been found to be successful for calculating optical extinction. We reject the small size bins as follows:

ASASP		CSASP
3 2 1 0	range	1 0
3 3 3 All	# of bins rejected	1 1

Note that we reject all data from ASASP range 0 because this full range is severely affected by ambiguity. This and rejection of the first bin in each CSASP range remove most ambiguity. The polynomial fit smoothing described below reduces the remaining ambiguity to an acceptable level.

Examples of the effects caused by the ambiguity zones are shown in Fig. 3. Shown are the results of PMS spectrometer sizing calibrations performed with the aerosol generator[3] at the Max-Planck Institute for Chemistry, Mainz, FRG. Results are shown for both the NPS spectrometers and the PMS spectrometers the Institute uses at Garmisch-Partenkirchen. The results show that the spectrometers size particles quite well except in the ambiguity zones regions where sizing is uncertain. We have had much less experience with the aircraft ASSP spectrometer. The results have shown that the best technique is to use all data except the first two bins of each size range. (Data from four other bins where there were electronic counting problems were also discarded.) The ambiguity zones did not appear to be a problem with this instrument.

III. Data Analysis

The two shipboard spectrometers count particles in six ranges with fifteen size bins per range for a total of ninety data points. These data are reduced to sixty-four points by the bin rejection scheme described above. Due to natural fluctuations, counting errors caused by electronic noise and ambiguity zones, the data are subject to uncertainties. Because of the uncertainties associated with individual points, an averaging technique is used to smooth the data for extinction calculations. This is done by using a seventh-order polynomial in $\log(dn/dr)$ vs $\log(r)$, where r is particle radius, dn is the number of counts per unit volume of air for a size bin, and dr is the width of the bin. The seventh order was subjectively selected by trial because it reproduces the major features of a spectrum and smooths out less credible variations. We chose a polynomial fit rather than a Deirmendjian, lognormal, etc., because we did not want the results to depend on the applicability of a particular physical model with only a few adjustable

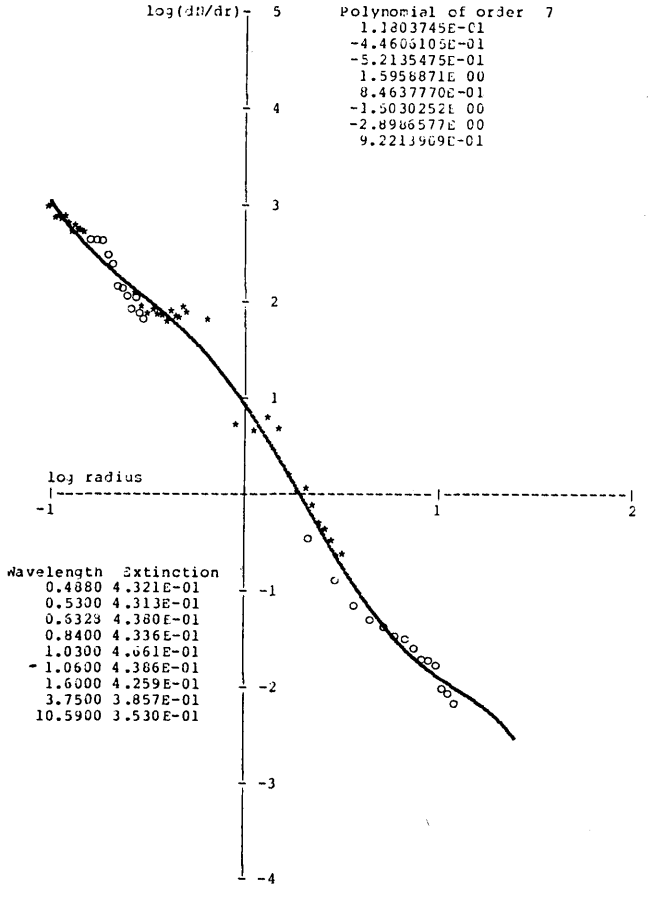

Fig. 4. Typical plot of $\log(dN/dr)$ vs $\log(r)$ data and the seventh-order polynomial fit (solid line).

parameters. A typical plot of the data and polynomial fit for a medium visibility day is shown in Fig. 4.

Because the highest-order term in a polynomial fit will always dominate at a large argument, a positive coefficient for the highest-order term will ultimately result in large positive $\log(dn/dr)$ for positive $\log(r)$ and vice versa for negative $\log(r)$. This turnover often occurs within the measured size region. We prevent this from occurring by generating two fictitious points outside the range of data at $\log(r) = \pm 1.5$, which are added to the data. These points are generated in the following manner: for -1.5 a linear extrapolation of the first five accepted points in the ASASP range 3 are used; for $+1.5$ a linear extrapolation of all points in the CSASP range 0 is used. The polynomial fit is calculated using all accepted data points and the two fictitious points.

Using this technique the polynomial fits are always of the quality shown in Fig. 4. Note, however, that because of the greater statistical scatter at large sizes the polynomial often is a poor extrapolation between the end of the data and the 1.5 generated point. This presents a special problem which will be discussed later in this paper.

Similar techniques are used for the aircraft spectrometer. The first eight accepted bins of range 3 are used to generate the point at -1.5 and all of range 0 for the point at $+1.5$. Because of the greater statistical scatter in the data from the aircraft probe and the greater range overlap, the polynomial fit is subject to occasional instabilities. When this occurs the fit bears no resemblance to the data, and such spectra are not included here.

Extinction calculations are performed by dividing the range $\log(r) = -1.0$ to $+1.5$ into increments of equal width of 0.05 in $\log(r)$. The average value of dn/dr for each increment is calculated from the fit to the data. The contribution to the scattering for each increment is determined using the appropriate Mie coefficient and the total extinction found by summing over all increments

$$\alpha(\lambda) = \sum_i Q_e(\lambda, r_i) \frac{dn}{dr_i} \pi r_i^2 \, dr_i,$$

where λ is the optical wavelength, Q_e the Mie extinction efficiency, and r_i the increment center radius. The extinction efficiencies are previously calculated as averages over each radius increment for each wavelength of interest and are accessed from a computer look-up table. The dependence of the index of refraction on wavelength used is the same as for LOWTRAN 3B.[4]

Because the contribution of the large size particles to the extinction is so great, the behavior of the fit in this range is critical. Note that the extinction calculation is carried out to $\log(r) = +1.5$ while the data ends at $+1.1$. In particular, if the polynomial fit has a large excursion between the end of the data and the added point at $+1.5$ and this portion of the fit is used in the calculation, the resulting extinction value will be seriously in error. The method developed for handling this problem will be described in Sec. IV.

IV. Extrapolation to Large Sizes

Let us first consider the question: Why extrapolate beyond the measured data at all? The reason is that we wish to use the aerosol data to calculate extinction for the full optical range visible through IR. Particles above 10-μm diam are very important in the IR range, even though there are relatively few of them. It is necessary to estimate the number of large particles beyond the measurement range or the extinction may be underestimated. Although one might argue that this extrapolation requires assumptions about the behavior of the spectrum that are not based on actual measurements in the region of interest, it should be realized that to cut off the extinction integral at $\log(r) = 1.1$ is equivalent to making the clearly unreasonable assumption that $dn/dr = 0$ for $\log(r) > 1.1$.

When examining aerosol data, volume plots are more useful than plots of number density. If the size range is large enough so that the Mie extinction efficiency is roughly constant, the extinction is proportional to $(dn/dr)A(r)dr$, where $A(r)$ is the particle cross-sectional area. Using volume $V \approx rA(r)$ and $dr/r = d(\log r)$, we see that the extinction is proportional to $(dV/dr)d(\log r)$. Thus a constant $\log(dV/dr)$ vs $\log(r)$ plot would show

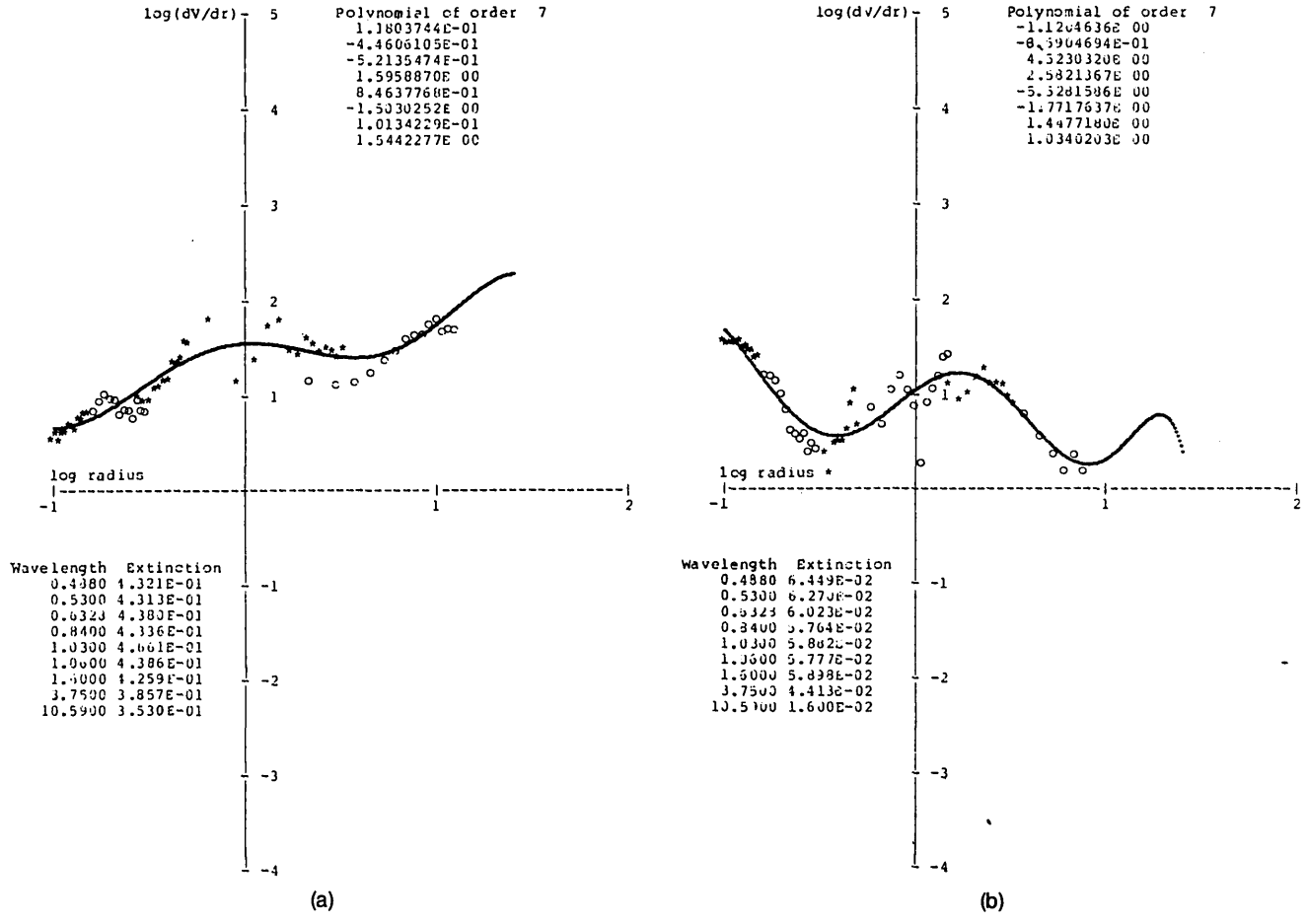

Fig. 5. Plots of $\log(dV/dr)$ vs $\log(r)$ for low visibility (a) and high visibility (b) cases. Solid lines are from the polynomial fits.

for large sizes a roughly constant contribution to extinction with size.

Volume plots for data obtained aboard the RV/Acania are shown in Figs. 5: (a) low visibility case and (b) high visibility case. [Note that Figs. 4 and 5(a) show the same data but that the last two polynomial coefficients are different. This is due to converting these coefficients to those appropriate for the volume plot.] Alternating symbols are used for the data points to delineate the different ASASP and CSASP ranges. The solid lines are the polynomial fits to the data. For the low visibility case the volume is continually increasing with radius so the large sizes make the major contribution to the extinction. For the high visibility case the large size particles' contribution to the extinction is a small fraction; the polynomial fit is poor at large sizes, but, since the large size contribution is small, the error introduced into the extinction will be small.

We have evaluated four extrapolation methods and tested them against optical measurements:

(1) Polynomial: Use the polynomial fit directly with no modification.

(2) Linear: The polynomial is terminated at the middle of the last range, and the remainder of the calculation uses a linear extrapolation from the termination point to the +1.5 end point.

(3) Constant: The polynomial is terminated at the radius of the last data point, and $\log(dV/dr)$ is assumed constant thereafter.

(4) Cutoff: The extinction calculation is cut off at the radius of the last data point.

We attempted to determine the best extrapolation method to use independent of validation with optical data. The conclusions listed in the following paragraph are based on the following assumption: without additional information it is unreasonable to assume that the extinction contribution from the extrapolation range is vastly different from the contribution from the adjacent sizes.

In this evaluation we have calculated the aerosol extinction at 0.4880 and 10.59 μm and the percent contribution to this extinction from the extrapolation range for the data shown in Fig. 5. The results are presented in Table I. When the visibility is low the extrapolation range is a major contributor to the extinction even in the visible. The polynomial and linear methods overestimate the extinction. The polynomial method overestimates seriously for cases where the visibility is low and

Table I. Total Aerosol Extinction and the Percent Contribution from the Extrapolated Size Ranges for Various Extrapolation Techniques

Technique	0.488 μm Extinction (km)	0.488 μm Percent contribution	10.59 μm Extinction (km)	10.59 μm Percent contribution
		Low visibility		
Polynomial	0.432	41	0.353	59
Linear	0.358	34	0.263	53
Constant	0.305	23	0.202	40
Cutoff	0.252	0	0.201	0
(Molecular)		(6)		(75)
		High visibility		
Polynomial	0.064	7	0.016	35
Linear	0.058	0.4	0.008	4
(Molecular)		(25)		(90)

[a] Results are presented for optical wavelengths of 0.4880 and 10.59 μm for low and high visibility cases. The percent contribution of molecular scattering and absorption to the total extinction is given in parentheses.

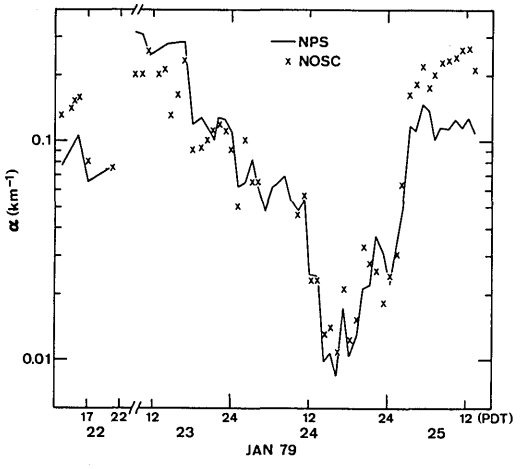

Fig. 6. Time history of the calculated aerosol extinction for the NPS (solid line) and NOSC (X) spectrometers. Data were collected coincidently during the NPS-NOSC intercomparison.

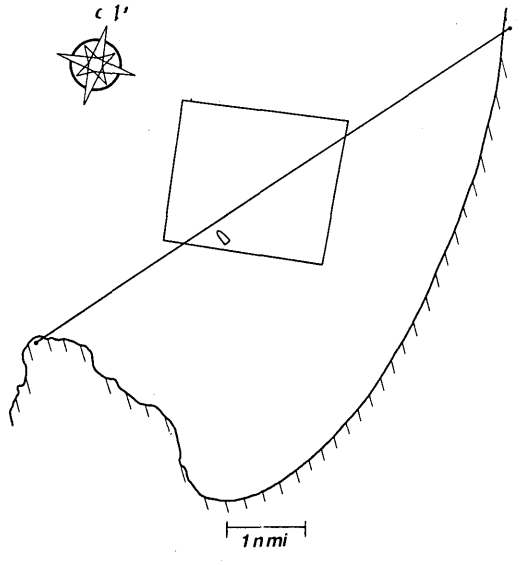

Fig. 7. MAGAT-80 experimental area on Monterey Bay. Solid line shows the 13-km optical path. Square shows ship operational area.

the fit has an excursion of the type shown in Fig. 5(b). The cutoff method always leads to underestimation. The constant method overestimates for high visibility and underestimates slightly for low visibility.

Table I also lists the percent contribution of the molecular scattering and absorption to the total extinction. One sees that at 10.59 μm the molecular component is dominant. This is fortunate since the calculation technique for aerosol extinction is most uncertain for the IR, where it is the smallest fractional contributor.

Errors will result for some circumstances whichever method or combination of methods is chosen. We have chosen a combination where the linear method is used when the slope of $\log(dV/dr)$ vs $\log(r)$ is less than or equal to zero for the last range (medium to high visibility) and where for the positive slope (low visibility) the constant method is used. Although some errors are introduced with this method, they are minimized, and it works quite well for predicting extinction, as will be shown in Sec. VII.

V. Spectrometer Intercomparison

Since the spectrometers used in this study are of different types they have been operated together for purposes of cross calibration. Two intercomparisons were performed before gathering the data reported here, and a third was performed during the experiment. A major intercomparison of several spectrometers, including those used for the work reported here, was performed on San Nicolas Island (SNI) in May 1979.[1] An additional side-by-side intercomparison of only the spectrometers used here was performed on top of a building, ~39 m (130 ft) above the sea surface, during January 1979.

The extinctions calculated from the measured aerosol spectra for the aircraft and shipboard systems are shown in Fig. 6. The comparison is very good over the 2½-day period except for a systematic difference of a factor of 2 during the morning of 25 Jan. High winds occurred (>10 m/sec) on that morning, but it is not known if the difference is associated with these winds. The SNI intercomparison (not shown here) showed acceptable agreement between the systems for a full 2-week period.

During the experiment reported here a series of flybys was made to compare ship and aircraft spetrometers. This was done in part because a new aircraft installation was being used and a year had passed since the last intercomparison. It was found necessary to make a correction because the spectrometers no longer agreed. Since the ship system has a wider range and better sensitivity, the aircraft system was corrected to the ship system for the data reported here. The comparison data used to determine this correction were not the data used in the comparisons with the optical results; it was a separate data set.

VI. MAGAT-80 Experiment

Investigators from NPS performed the Marine Aerosol Generation and Transport (MAGAT) experiment on Monterey Bay from 28 Apr. to 9 May 1980.[5] The Environmental Physics Group performed extensive meteorological and aerosol measurements on the RV/ACANIA and the Airborne Research Associates aircraft. The Optical Propagation Group conducted overwater optical propagation measurements. The purpose of the experiment was to validate models for optical extinction and scintillation with coincident optical, meteorological, and aerosol measurements. The scintillation results have already been reported.[6]

The experimental area including the optical path and ship location are shown in Fig. 7. During the 2-week period 105 h of optical data, 37 h of coincident optical and shipboard data, and 20 fly-overs of the optical path were obtained. The ship was positioned as shown in the figure and performed ½-h time average measurements. The optical and aircraft measurements were path averages. The shipboard measurements were not sampling the same air as the aircraft and optical range because of the prevailing wind. However, measurements were made during times of prevailing sea breezes when reasonable horizontal homogeneity existed.

VII. Results

The results are comparisons between extinction coefficients calculated from measured aerosol spectra and optically measured extinction coefficients. Results are shown both as time histories and as scatter plots. The procedures outlined in the preceeding sections were used to process the aerosol data. Several factors affect the accuracy of the spectrometers:

(1) the differences (unknown) between the assumed and actual particle indices of refraction;

(2) the smoothing of the measured aerosol distribution;

(3) the procedures for extrapolating beyond the measured size.

It is not possible to separate the effects due to these factors. The first two will contribute to errors for all conditions, while the last will be most important at low visibility and also at long optical wavelengths. We must emphasize here that the bin rejection and extrapolation techniques were developed independent of comparisons with optical data.

To compare measured optical extinction and values calculated from aerosol spectra, molecular extinction must be taken into account. (The wavelengths used were selected to minimize this correction.) The molecular components were calculated using LOWTRAN IIIB[4] and subtracted from the optically measured extinction to leave only the aerosol extinction. This was then compared with the values calculated from the ship and aircraft aerosol data. The meteorological parameters (temperature and relative humidity) most correlated to molecular extinction were relatively constant over the period of the experiment. Therefore, the following molecular extinction values were used for all data:

Wavelength (μm)	0.63	0.84	1.03	1.06
Molecular (km^{-1})	0.01	0.04	0	0

A time history of optical and shipboard measured aerosol extinction for 1.06 μm is shown in Fig. 8. The extinction varied from 0.5 to 0.02 km^{-1} and showed considerable variation within any given day. Measurement periods generally lasted from 2 to 4 h, and the extinction would typically change by a factor of 2 during a period. On 2 May measurements were obtained over a full 20-h period. The extinction varied by slightly more than a factor of 2 both on the long term and over periods as short as 2 h. As can be seen from the figure, the agreement between the optical and shipboard aerosol measurements is excellent. The only serious disagreement was on 4 May when one comparison was off by a factor of almost 3.

A scatter plot comparison of coincident aircraft and optical extinction values is shown in Fig. 9. Data are shown for 0.63, 0.84, and 1.06 μm for the 20 fly-bys. The solid line indicates perfect agreement. Out of the 20 runs only two calculated values disagree with the optical results by more than a factor of 2. The average ratio for aerosol vs optical data is 1.0 + 50%, −40%. This agreement is quite good since it is well within the accuracy needed to predict the performance of most electro-optic systems.

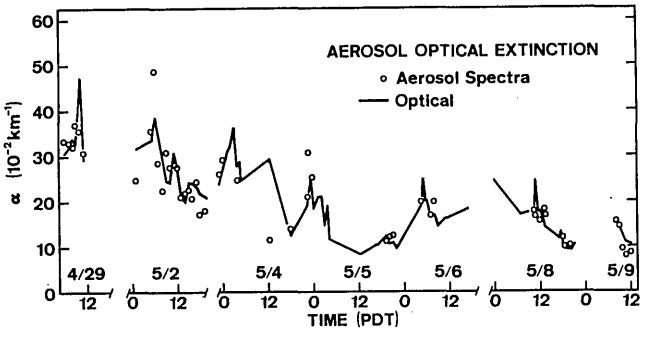

Fig. 8. Time history of aerosol extinction calculated from shipboard aerosol data and measured optically for 1.06-μm wavelength.

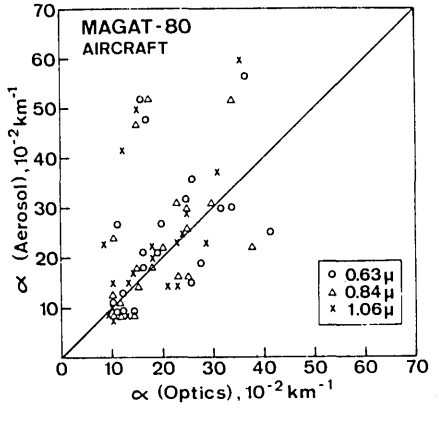

Fig. 9. Scatter plot of aerosol extinction calculated from aircraft aerosol data and measured optically.

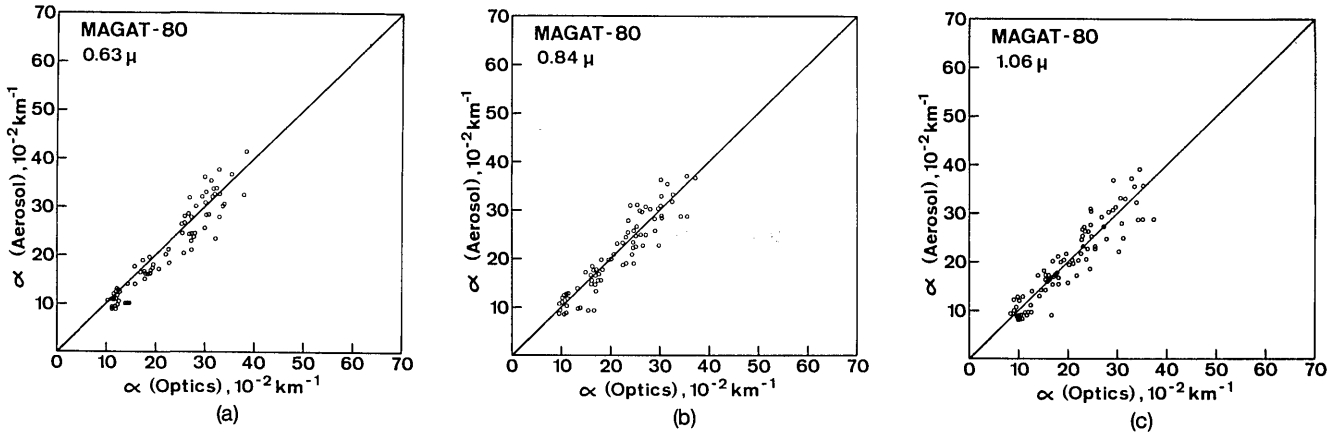

Fig. 10. Scatter plots of aerosol extinction calculated from shipboard aerosol data and measured optically for (a) 0.63-, (b) 0.84- and (c) 1.06-μm wavelengths.

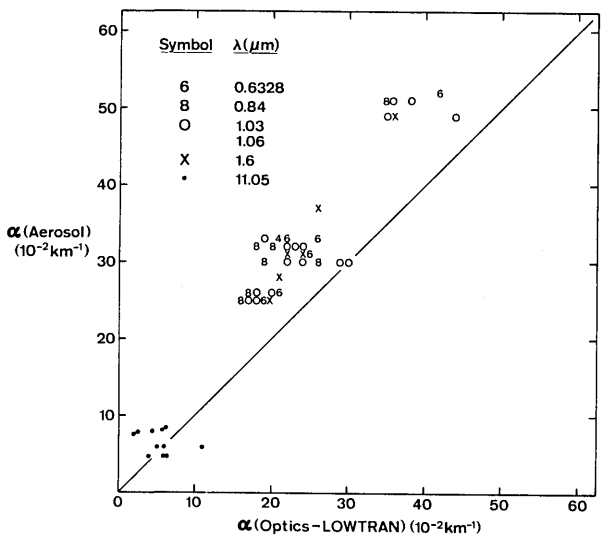

Fig. 11. Scatter plot of aerosol extinction calculated from shipboard aerosol data and measured optically during the CTQ-79 operation.

Scatter plot comparisons of the shipboard aerosol–optical extinctions for 0.63, 0.84, and 1.06 μm are shown in Fig. 10. Assuming the optical results to be correct, only two data points for 0.84 μm and one at 1.06 μm show an error >50%. The average errors are +10%, −20% for all wavelengths. This is exceptional agreement, better than can be expected for all except the most carefully performed scientific experiments.

Previous to MAGAT-80, NPS performed humidity fluctuation experiments on Monterey Bay (CTQ-79). Preliminary aerosol and optical measurements were performed at that time, and we show the results in Fig. 11 because optical measurements at additional wavelengths (1.6 and 11 μm) were performed. For these results the computed extinctions were systematically high by ~40% for all wavelengths. The agreement at 11 μm is remarkable in view of the fact that molecular extinction is dominant and the optical result is obtained by subtracting two large numbers (total − molecular). The CTQ-79 results are more representative of the magnitudes of error to be expected for most field programs.

These results show that aerosol distributions obtained from optical aerosol spectrometers can be confidently used to calculate optical extinction. With reasonable care one can expect accuracy to within 40%. Since a single spectrometer probe is typically useful for about one particle size decade, it is unlikely that a single- (or even double-) probe system will cover the full particle size range of relevance. For such cases it is important that extrapolation be used in the data analysis so that all sizes that potentially contribute to the extinction will be included.

The authors take this opportunity to thank the Naval Ocean Systems Center for the use of their airborne aerosol spectrometer and for providing intercomparison data. We also thank the NPS Optical Propagation Group for making their data available. The cooperation of Ralph Markson and Jan Sedlacek of Airborne Research Associates is also acknowledged. The Max-Planck Institute for Chemistry, Mainz gave welcome assistance in performing calibrations.

References

1. D. Jensen, R. Jeck, G. Trusty, and G. Schacher, "Intercomparison of PMS Particle Size Spectrometers," Naval Ocean Systems Center, TR 555.
2. R. G. Pinnick, and H. J. Auvermann, J. Aerosol Sci. **10**, 55 (1979).
3. R. Jaenicke, J. Aerosol Sci. **3**, 95 (1972).
4. J. E. A. Selby, E. P. Shettle, and R. A. M. Clatchey, "Atmospheric Transmittance from 0.25 to 28.5 μm: Supplement LOWTRAN 3B (1976)," Air Force Geophysical Laboratory TR-76-0258.
5. E. C. Crittenden, E. A. Milne, A. W. Cooper, G. W. Rodeback, and S. H. Kalmbach, "Overwater Optical Scintillation Measurements During MAGAT-80," NPS-61-80-018.
6. K. L. Davidson, G. E. Schacher, C. W. Fairall, and A. Goroch, Appl. Opt. **20**, 2919 (1981).